Electronic Supplementary Material (ESI) for Inorganic Chemistry Frontiers.


# Supplementary material

# A self-calibrating bimetallic lanthanide metal-organic luminescent sensor integrated with logic gate operation for detecting N-methylformamide

Si-Jia Qin, Xianglong Qu and Bing Yan*

*China-Australia Joint Laboratory of Functional Molecules and Ordered Matters, School of Chemical Science and Engineering, Tongji University, Shanghai 200092, China*

* Corresponding author Email addresses: byan@tongji.edu.cn (Bing Yan)

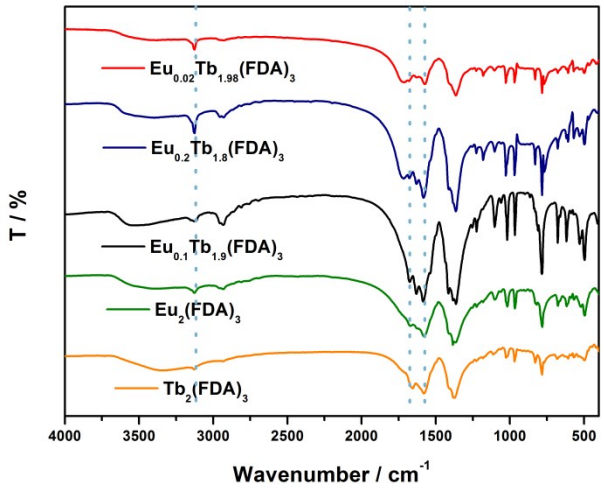


**Figure S1**. The FT-IR images of $Eu_xTb_{2-x}(FDA)_3$. The peaks around 3000 $cm^{-1}$ were attributed to the O-H vibration. The peaks around 1680 $cm^{-1}$ were C=O stretch, which were extremely weak owing to the coordinating with lanthanide ions.

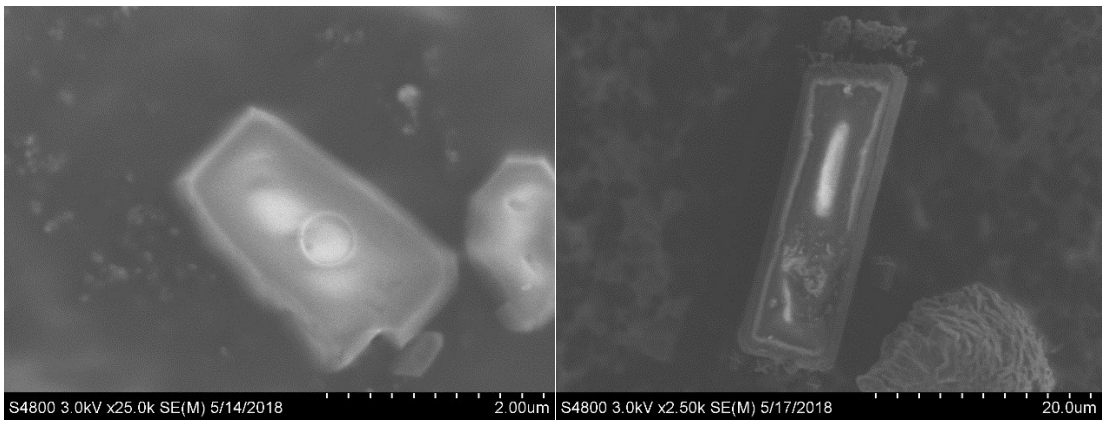


**Figure S2.** SEM images of $Eu_{0.1}Tb_{1.9}$ $(FDA)_3$.

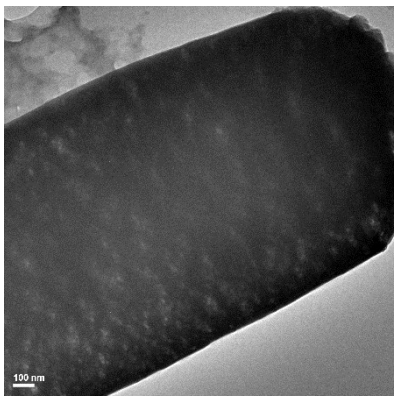


**Figure S3.** TEM images of $Eu_{0.1}Tb_{1.9}(FDA)_3$.

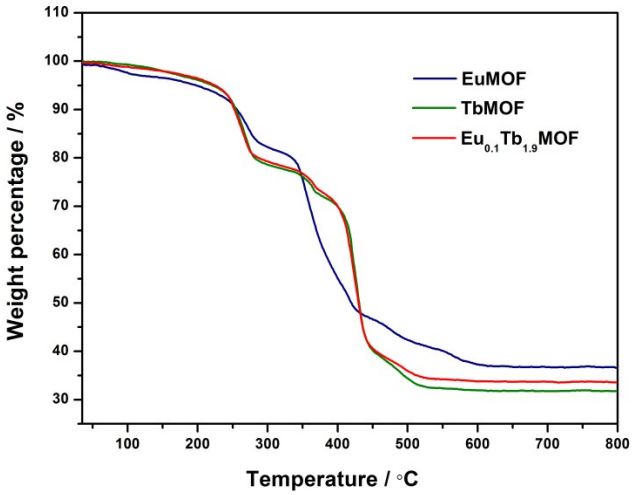


**Figure S4.** Thermal gravimetric analysis curves for Eu-MOF, Tb-MOF, and $Eu_{0.1}Tb_{1.9}$-MOF

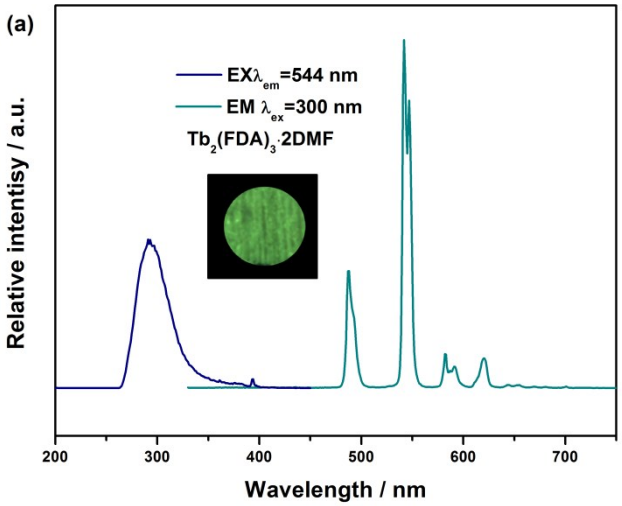

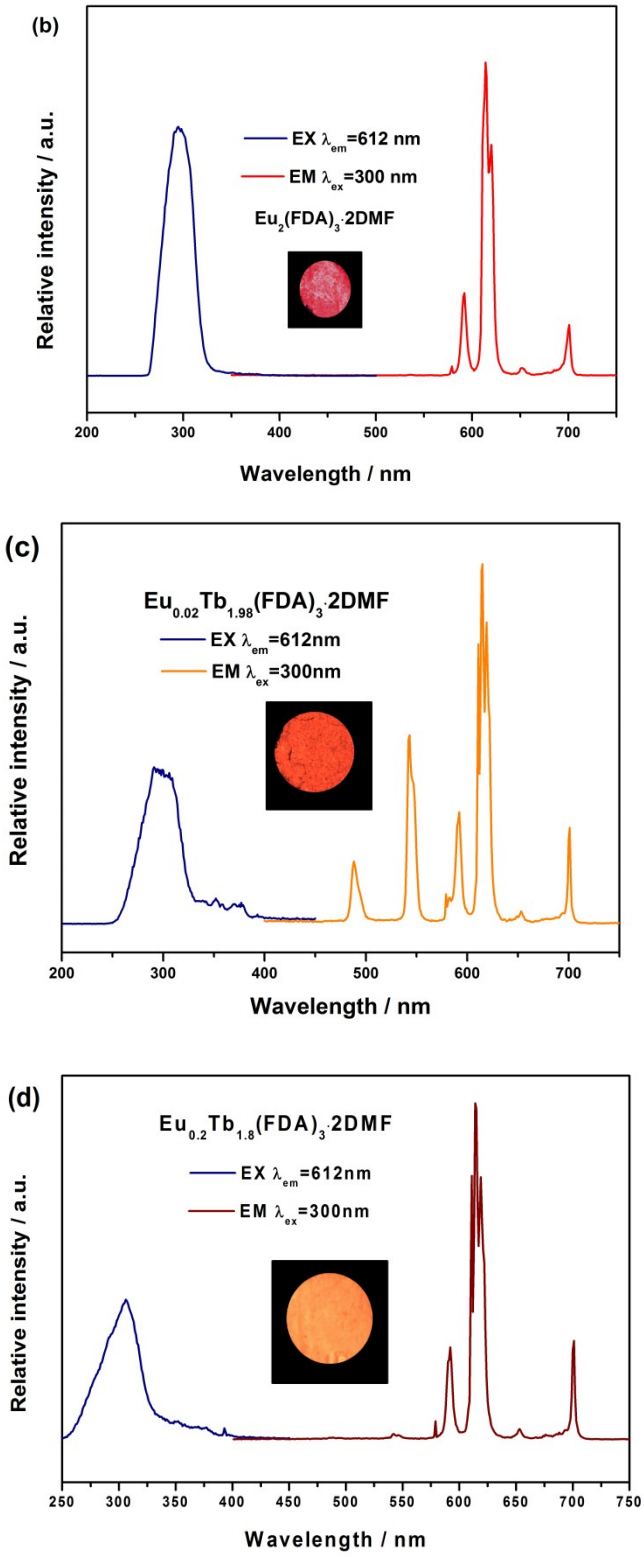


**Figure S5.** The spectra of (a) $Tb_2(FDA)_3$, (b) $Eu_2(FDA)_3$, (c) $Eu_{0.02}Tb_{1.98}(FDA)_3$, and (d) $Eu_{0.2}Tb_{1.8}(FDA)_3$ in solid-state, inset shows the powder under UV-light irradiation.

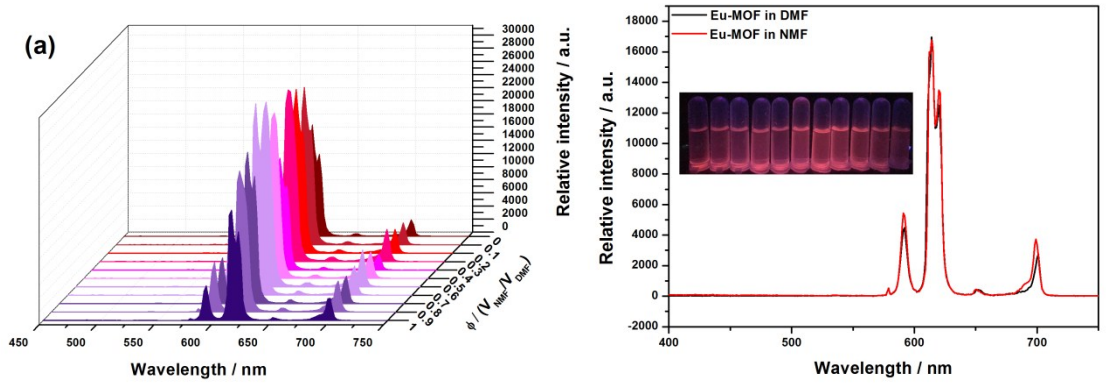
(a)
Wavelength / nm
Relative intensity / a.u.
ϕ / (V_NMF / V_DMF)
Eu-MOF in DMF
Eu-MOF in NMF
Relative intensity / a.u.
Wavelength / nm

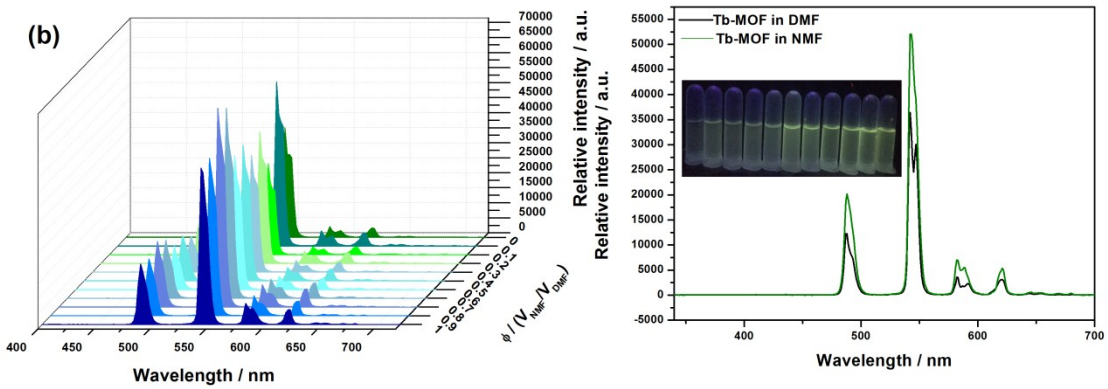
(b)
Wavelength / nm
Relative intensity / a.u.
ϕ / (V_NMF / V_DMF)
Tb-MOF in DMF
Tb-MOF in NMF
Relative intensity / a.u.
Wavelength / nm

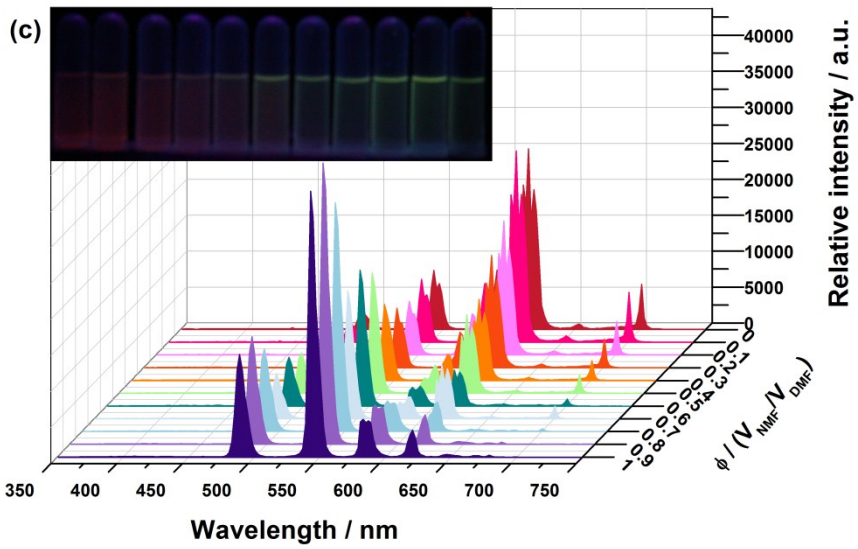
(c)
Wavelength / nm
Relative intensity / a.u.
ϕ / (V_NMF / V_DMF)

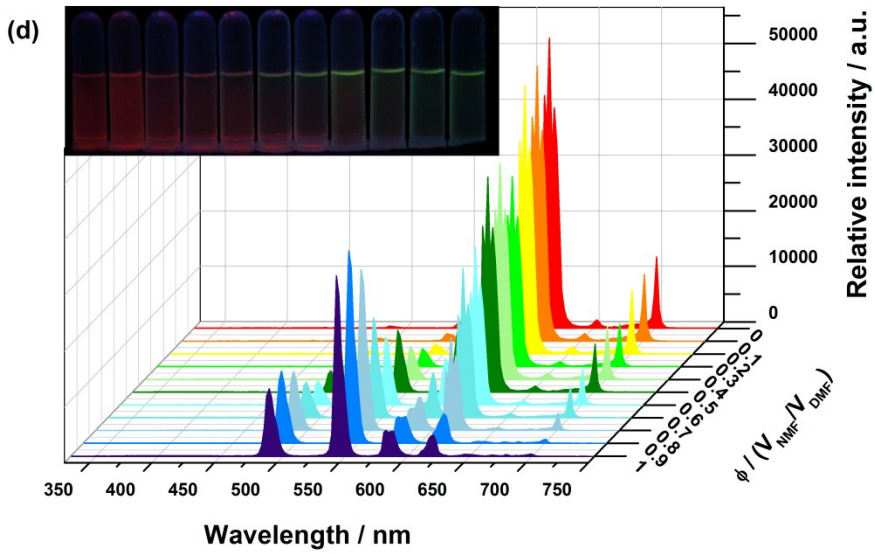


**Figure S6.** The suspension-state luminescent spectra of (a) $Eu_2(FDA)_3$, (b) $Tb_2(FDA)_3$, (c) $Eu_{0.02}Tb_{1.98}(FDA)_3$, and (d) $Eu_{0.2}Tb_{1.8}(FDA)_3$ within different volume content of NMF in DMF from 0 to 1, excited at 300 nm at RT.

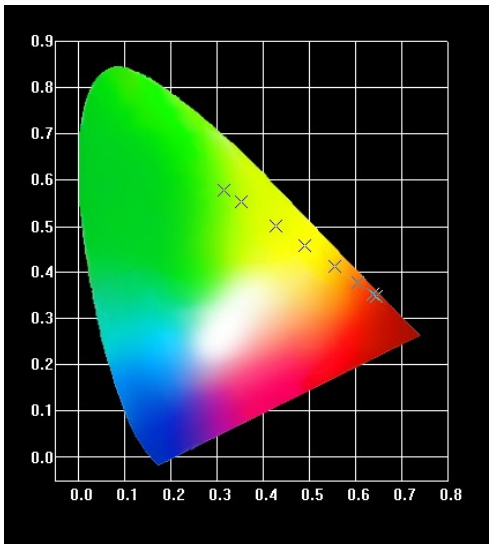


**Figure S7.** The CIE chromaticity diagram shows the change at different volume ratios of NMF.

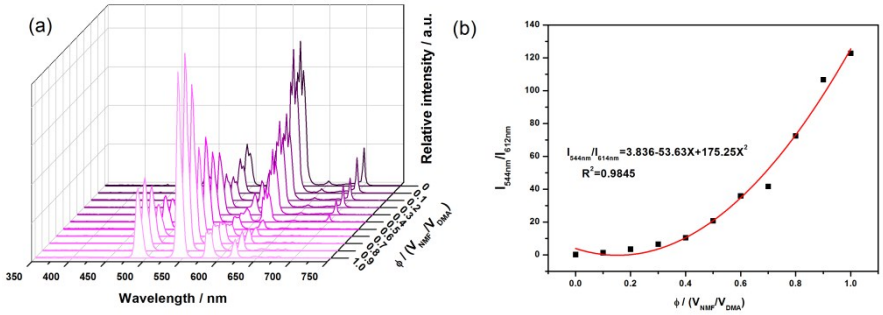


**Figure S8.** The (a) suspension-state luminescent spectra and (b) the corresponding curve ($I_{544nm}/I_{614nm}$=3.836-53.63X+175.25X$^2$, $R^2$=0.9845) of the probe in different volume content of NMF in DMA from 0 to 1.

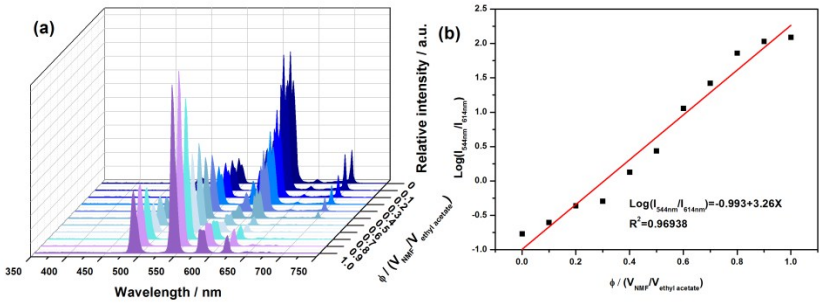


**Figure S9.** The (a) suspension-state luminescent spectra and (b) the linear model (Log($I_{544nm}/I_{614nm}$)=-0.993+3.26X, $R^2$=0.969) of the sensor in different volume content of NMF in ethyl acetate from 0 to 1, excited at 300 nm at RT.

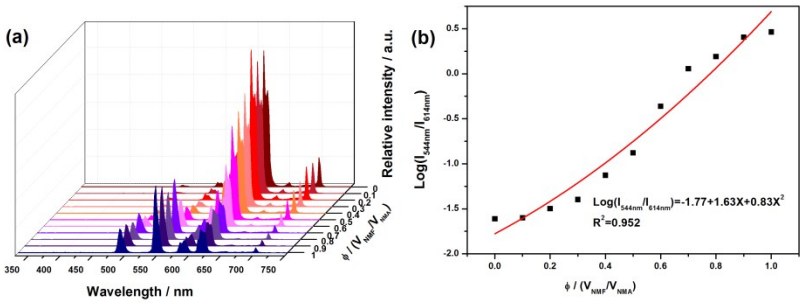


**Figure S10.** The (a) suspension-state luminescent spectra and (b) the normalization curve (Log($I_{544nm}/I_{614nm}$)=-1.77+1.63X+0.83X$^2$, $R^2$=0.952) of the sensor in N-Acetyl-N-Methylamine (NMA) different volume content of NMF in from 0 to 1, excited at 300 nm at RT.

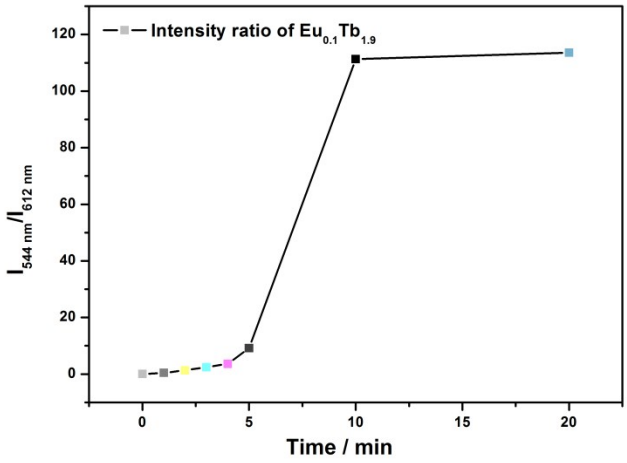


**Figure S11.** The integrated intensity ratio of the $Eu_{0.1}Tb_{1.9}(FDA)_3$ changed with the contact time of NMF.

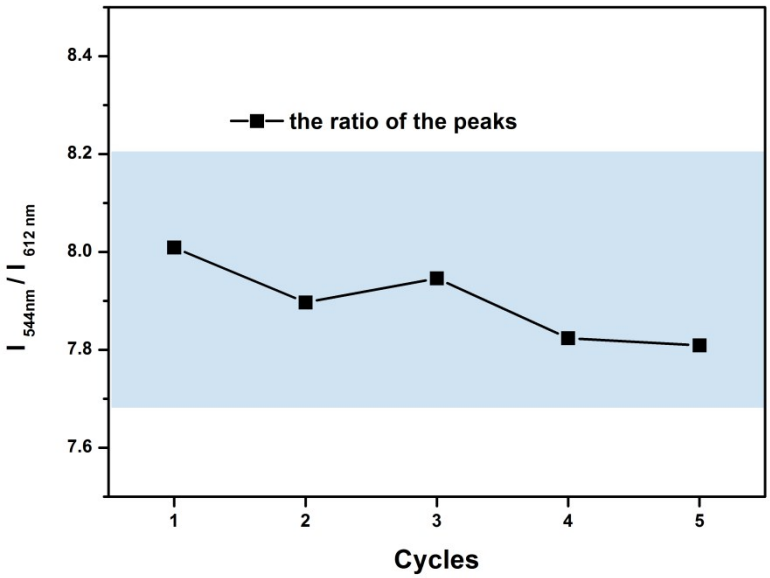


**Figure S12.** Integrated intensity ratio $I_{544nm}/I_{612nm}$ of $Eu_{0.1}Tb_{1.9}(FDA)_3$ in the solvents for five runs.

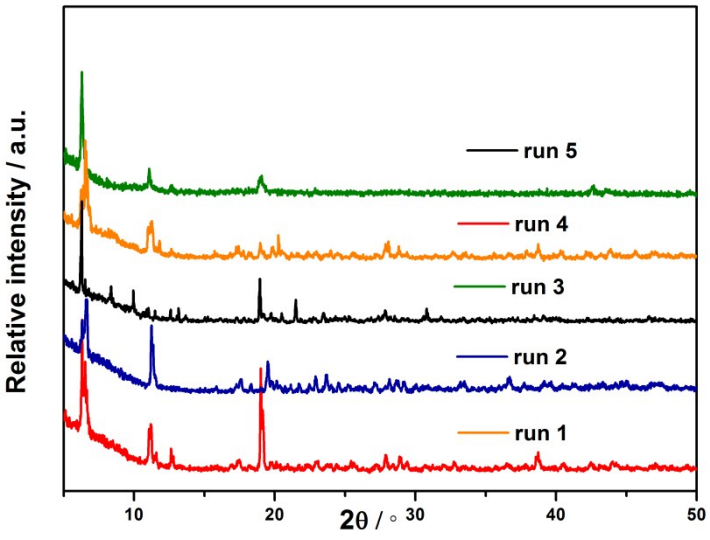


**Figure S13**. The XRD patterns of $Eu_{0.1}Tb_{1.9}(FDA)_3$ after five runs.

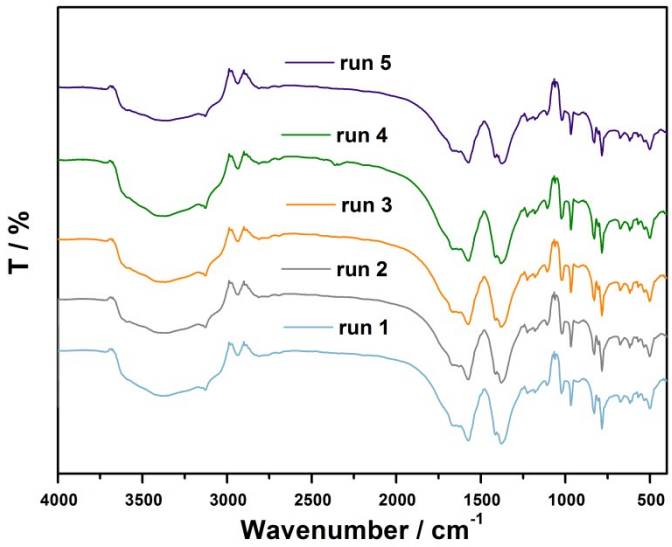


**Figure S14**. The IR patterns of the sensing probe after cycling.

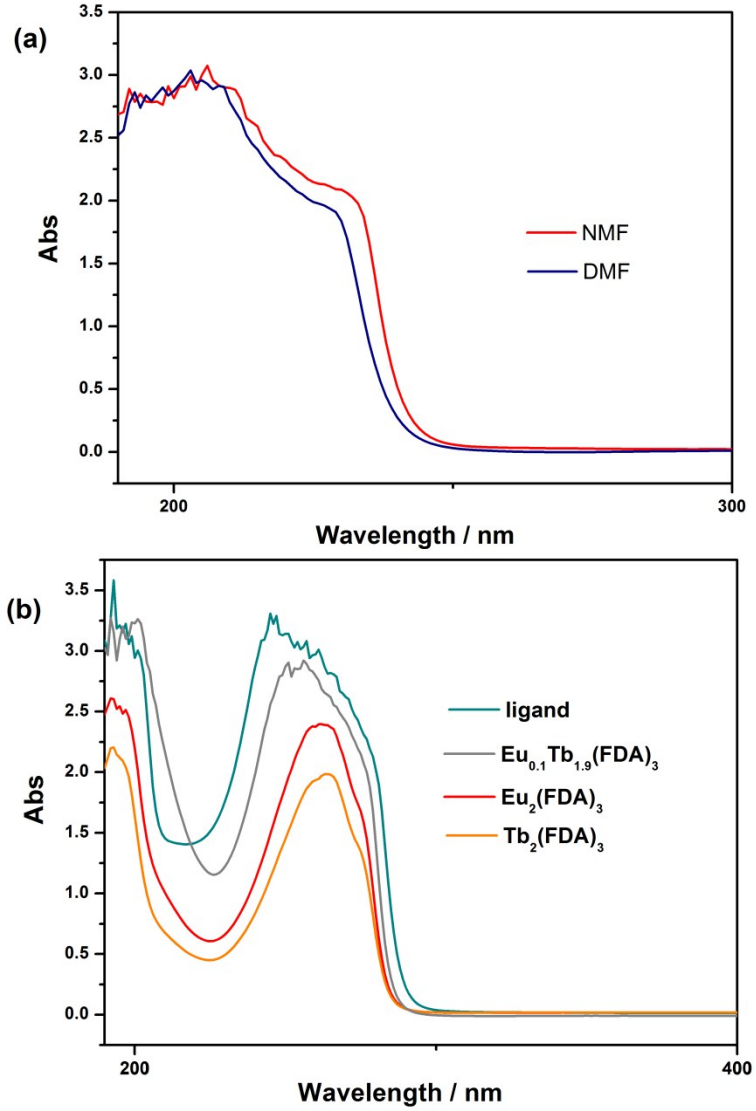


**Figure S15.** UV-vis spectra of (a) DMF and NMF; (b) ligand, and MOF.

**Table S1.** The ICP analysis result of mixed $Eu_xTb_{1-x}$-MOF.

| LMOF | Eu(mg/L) | Tb(mg/L) | Ratio | Ratio in theory |
|---|---|---|---|---|
| **$[Eu_{0.02}Tb_{1.98}(FDA)_3(DMF)_2]\cdot 2DMF$** | 0.736 | 49.65 | 0.0148 | 0.0101 |
| **$[Eu_{0.1}Tb_{1.9}(FDA)_3(DMF)_2]\cdot 2DMF$** | 3.815 | 91.10 | 0.0418 | 0.0526 |
| **$[Eu_{0.2}Tb_{1.8}(FDA)_3(DMF)_2]\cdot 2DMF$** | 5.394 | 56.84 | 0.0949 | 0.111 |

**Table S2.** Performances of different sensor systems for detection of NMF.

| Sensor system | Linear range | Advantage | Disadvantage | Ref |
|---|---|---|---|---|
| Liquid chromatography-mass spectrometry (LC-MS) | 0.004-8 μg/mL | Accurate, and reliable. | Complicated process. | 1 |
| Gas chromatography-mass spectrometry (GC-MS) | 0.3-30 μg/mL | Non-invasive, and reliable. | Requiring highly skilled personnel to operate. | 2 |
| Eu@MOF-1 | 0-100 μM | Fast response, and high selectivity. | Monometallic MOF, non-self reference. | 3 |
| $[Eu_{0.1}Tb_{1.9}(FDA)_3]$ | 0-100% | Self-calibrating, visibility and good reusability. | Preliminary test. | This work |

**Table S3.** Luminescence lifetimes of sensor $Eu_{0.1}Tb_{1.9}$ $(FDA)_3$ with excitation at 300 nm in different volume ratio of NMF.

| **The ratio of NMF** | **$^5D_4$ of $Tb^{3+}$/μs** | **$^5D_0$ of $Eu^{3+}$/μs** | **η** |
|---|---|---|---|
| **0** | 69 | 1528 | 0.96 |
| **0.1** | 100 | 1512 | 0.94 |
| **0.2** | 218 | 1511 | 0.87 |
| **0.3** | 331 | 1457 | 0.80 |
| **0.4** | 549 | 1487 | 0.66 |
| **0.5** | 1375 | 1706 | 0.15 |
| **0.6** | 1377 | 1476 | 0.15 |
| **0.7** | 1446 | 1449 | 0.11 |
| **0.8** | 1436 | - | 0.10 |
| **0.9** | 2436 | - | - |
| **1** | 1425 | - | 0.1 |


1. J. H. Sohn, M. J. Han, M. Y. Lee, S. K. Kang and J. S. Yang, *J. Pharm. Biomed. Anal.*, 2005, **37**, 165-170.
2. V.-S. Wang and M.-Y. Lu, *J. Chromatogr. B:Anal. Technol. Biomed. Life Sci.*, 2009, **877**, 24-32.
3. N. Sun and B. Yan, *Sens. Actuators, B*, 2018, **261**, 153-160.